BIOLOGY OF REPRODUCTION 39, 105–118 (1988)

The Consequences of Actin Disruption at Sertoli Ectoplasmic Specialization Sites Facing Spermatids after in Vivo Exposure of Rat Testis to Cytochalasin D[1]

LONNIE D. RUSSELL,[2,3] JANE C. GOH,[3] RASHED M. A. RASHED,[3] and A. WAYNE VOGL[4]

Department of Physiology[3]
School of Medicine
Southern Illinois University
Carbondale, Illinois 62901-6512
and
Department of Anatomy[4]
Faculty of Medicine
University of British Columbia
Vancouver, British Columbia
Canada V6T 1W5

ABSTRACT

Cytochalasin D (CD) was used to perturb actin filaments of the Sertoli ectoplasmic specialization (ES)—a cytoskeletal complex of the Sertoli cell related to spermatids. CD (500 μM for 6 h) produced a loss of 88% of the ES facing the head region of early (Step 8) elongating spermatids as compared to vehicle (dimethylsulfoxide:saline) controls. Nitrobenzoxadiazole-phallacidin staining of F-actin revealed a CD-related loss of uniform fluorescence over the head of elongated spermatids. To examine for a possible relationship between the presence of actin and cell attachment at ES sites, hypertonic fixatives were introduced to provoke cell shrinkage and stress ES-associated junctions. After osmotic stress, cell-to-cell adhesion at ES sites remained intact in vehicle-treated animals. CD treatment caused Sertoli cells to separate from elongating spermatids at sites where ES had been lost from the Sertoli cell surface. It is suggested that actin of the ES plays a role in cell-to-cell interaction analogous to its possible role at the Sertoli cell barrier. In CD-treated animals, structures resembling tubulobulbar complexes frequently developed at sites where ES was lost, suggesting that the loss of ES has a facilitatory role in tubulobulbar complex formation. It is hypothesized that tubulobulbar complexes are devices that rid the cells of ES-associated junctional links to effect dissociation of the spermatid from the Sertoli cell during spermiation.

Spermatids at Step 8 of development are known to become oriented with their acrosomes facing the base of the Sertoli cell. After CD treatment, a 5.8-fold increase in malorientation of Step 8 spermatids was noted. A role for the ES cytoskeletal complex in orienting the spermatid acrosome toward the basal aspect of the Sertoli cell is also suggested.

INTRODUCTION

As spermatids begin their elongation phase of development, a region of tight adhesion occurs between Sertoli cells and these spermatids where the acrosome comes in close apposition to the spermatid cell surface (Russell, 1977; Romrell and Ross, 1979; Russell and Peterson, 1985). That the adhesion is trypsin-sensitive (Romrell and Ross, 1979) indicates that a proteinaceous substance links the two cells, although there is only meager morphological evidence to demonstrate the linking entities (Russell and Peterson, 1985). These junctions, for which no name has been given, are poorly investigated, yet are found in all mammals studied to date.

At the surface of the Sertoli cell is a surface cytoskeletal complex that is topographically related to this trypsin-sensitive junctional region. Composed of hexagonally packed actin filament bundles (Toyama, 1976; Franke et al., 1978) and more deeply positioned endoplasmic reticulum (Flickinger and Fawcett, 1967; Nicander, 1967; Masri et al., 1987), it has been called the "ectoplasmic specialization" (ES;

Accepted February 10, 1988.
Received October 23, 1987.
[1] This work was supported by PHS HD 20300 (L.D.R.) and MRC MT-8020 (A.W.V.)
[2] Reprint requests.

Russell, 1977). There are numerous functions proposed for the Sertoli spermatid ES (Ross and Dobler, 1975; Gravis et al., 1976; Russell, 1977; Fawcett, 1979; Romrell and Ross, 1979; Russell and Peterson, 1985; Vogl et al., 1986; Masri et al., 1987; Sprando and Russell, 1987), but virtually no solid data to indicate whether or not the ES participates in, or is related in any way other than topographically to, the cell-to-cell adhesion that occurs between plasma membranes at ES sites.

The present study was undertaken to demonstrate linking elements of the ES and to perturb the actin filaments of the ES to determine if there is a relationship between actin comprising the ES and the property of cell-to-cell adhesion seen at ES sites. The opportunity was also available to examine other proposed functions for ES which include a potential role of ES in orienting spermatids.

MATERIALS AND METHODS

Intratesticular Injection

The method of Russell et al. (1986) was used to inject 50 μl of vehicle (1 dimethylsulfoxide [DMSO] : 1 saline) or cytochalasin D (CD) dissolved in vehicle into the testis of sodium pentobarbital-anesthetized animals. Specific details as to the concentration of CD used and interval after injection until animals were killed are provided in the Results section.

Standard Tissue Preparation

Adult, male Sprague-Dawley rats weighing 250–440 g were used. Cytochalasin D and vehicle were prepared according to the method of Weber et al. (1988). Fifteen minutes prior to initiation of perfusion-fixation, heparin (100–130 I. U. per 100 g body weight) was injected i.p. (Russell et al., 1986a). Perfusion-fixation consisted first of clearing the testis with saline (0.9%), then primary fixation using 5% buffered (0.05 M sodium cacodylate; pH 7.4) glutaraldehyde for 45 min. Testes were removed, diced in fixative, and washed overnight in buffer. Post-fixation consisted of osmium (1%):ferrocyanide (1.25%) treatment, according to Russell and Burquet (1977), or simply osmium (1%) treatment for 1 h, whereupon tissues were dehydrated in a graded series of ethanol, cleared with propylene oxide, and infiltrated and embedded in Araldite (CY212; Polysciences, Warrington, PA). Thick sections (<1 μm) were made with an ultramicrotome (Hitachi Sci. Inst., Mountain View, CA) and areas of the block showing appropriate stages of the cycle (Leblond and Clermont, 1952) were trimmed for examination of ultrathin sections on a Hitachi (H500H, Hitachi Sci. Inst.) electron microscope. For morphometric procedures, sections were mounted on Formvar (Polysciences)-coated grids, micrographs were taken at original magnification of 1600×, and montages were made of entire tubular cross-sections. The final magnification of micrographs was 2650×.

Cytoskeletal Preparations

Cytoskeletal preparations were made to examine the junctional properties at ES sites. Blood was cleared from the testis by a 5-min perfusion through the testicular artery with phosphate-buffered saline (PBS) made according to Vogl and Soucy (1985) containing 5 mM ethylenediaminetetraacetate (EDTA). Testes were removed, decapsulated, immersed in 20 mM EDTA/PBS (5 min) and minced with a razor blade in 5 mM EDTA/PBS. Testis fragments were syringe-plunged first with an 18-1/2-gauge needle and subsequently with a 23-gauge needle. An aliquot was subsequently centrifuged to obtain a 1-mm-thick pellet. The pellet was fixed (1.5 h) in 3% glutaraldehyde containing 1% Triton X-100 (wt/vol) in 0.05 M cacodylate buffer (pH 7.4) containing 50 mM L-lysine and 5 mM EDTA. The pellet was fixed (1.5 h) in the same solution without detergent or lysine. The pellet was washed in 4°C 0.05 M barbitol buffer (pH 7.6) for 30 min, fixed in 1% osmium tetroxide in barbitol buffer (pH 7.6) for 15 min on ice, rinsed in 4°C water (three times), and stained with 2% uranyl acetate (in 4°C water) in the dark overnight. Subsequent dehydration and infiltration was according to the procedure described above.

Tissue Preparation Using Hypertonic Fluids

Hypertonic fluids were used to provoke tissue shrinkage to determine sites of cell-to-cell adhesion. Dextrose (10-20%) was added to the glutaraldehyde perfusate of four animals. In two identical experiments, tonicity-related shrinkage stresses were provoked in vitro after decapsulation of the testis and isolation of small seminiferous tubule fragments. These fragments were exposed to a primary fixation employing glutaraldehyde with and without the addition of dextrose (10–20%). Finally, some tissues

were exposed to hypertonic dextrose (10–20%) 5 min prior to perfusion of the fixative described above. Spermatids at late Step 8 through Step 11 of spermiogenesis were selected to determine the effect of osmotic stress.

Morphometry

From whole, tubular cross-sections reconstructed, as described above (see Standard Tissue Preparation above), Step 8 spermatids at late Stage VIII of development were selected to measure both the length of the acrosome (in section) and the length of the ES (in section) which corresponded to the acrosomal region of the spermatid. Length was determined by a Numonics 1224 (name of supplier, Lansdale, PA) electronic digitizer. The total ES length was divided by the total acrosomal length and expressed as a mean percentage of ES per spermatid displaying (in section) an acrosome. The data were gathered from two montages of vehicle (dimethylsulfoxide [DMSO]for 6 h)-treated (214 total spermatids with acrosomes visible) and four montages of CD-treated (500 μM for 6 h) animals (531 total spermatids with acrosomes visible).

Orientation of Step 8 (late Step 8) spermatids was determined by the following method. Spermatids were considered to be oriented normally when the central elevation of their acrosomes faced the most proximal aspect of the basal lamina or 90° either side (left or right as viewed in section) of this position. Malorientation of spermatids was judged to occur when the central point of the acrosome faced the tubular lumen or up to 90° to the left or right of this position. It was not necessary to visualize the central region of the acrosome in all cases, since its position could be surmised from visualization of a portion of the acrosome. The number of maloriented spermatids was expressed as a percentage of total acrosome-visible spermatids for which the orientation could be determined. The spermatids utilized to determine orientation were those used to measure ES (see above).

Preparation of Epithelial Sheets

Epithelial sheets were prepared to isolate cells for staining of filamentous actin. The technique of Vogl and Soucy (1985), as modified by Russell et al. (1986b) and Weber et al. (1988), was utilized to isolate epithelial sheets. Epithelial sheets were incubated with nitrobanzoxadiazole (NBD)-phallacidin (NBD-P) according to Vogl and Soucy (1985) and examined on a Zeiss Photomicroscope II (Nikon Instru., Garden City, NY) and a Nikon Optiphot Microscope (Nikon Instr., Garden City, NY). In some instances, phase photomicrographs corresponding to the field of fluorescence micrographs were taken of epithelial sheets and Sertoli-germ cell fragments.

RESULTS

Using standard tissue preparation techniques (see Methods), we could identify ES in either uninjected or vehicle-treated animals from an accumulation of subsurface actin filaments of the Sertoli cell, which faced the acrosomal region of the elongating spermatid, as well as endoplasmic reticulum, which lay on the deep aspect of the filaments. The entire complex extended from 80 to 160 nm of the cell surface (Fig. 1 and inset). Occasional filamentous elements were seen to bridge the intercellular space, although these were poorly visualized (Fig. 1 and inset). The presence of ES facing each spermatid was first noted at early to mid Step 8 of development; by late Step 8, ES occupied virtually all of the region overlying the acrosome. As has been shown previously (Russell et al., 1980), ES remained until Step 19 of spermiogenesis and was resorbed focally prior to and during the period of tubulobulbar complex formation. Cytoskeletal preparations treated with lysine and with uranyl acetate en bloc after partial triton extraction emphasized the actin filaments overlying the heads of elongate(ing) spermatids and also revealed linking elements between the spermatid and Sertoli plasma membranes at ES sites. These elements were estimated to be about 2–3 nm in diameter and about 7–10 nm long, and, as such, spanned the entire width of the intercellular space (Fig. 2 and inset).

After treatment with CD (300–500 μM for 30 min to 6 h), standard tissue processing revealed that ES was partially lost from its position facing elongate(ing) spermatids at all steps of spermatid development (Figs. 3–5). The vehicle-treated animals did not manifest ES loss (see morphometry below) but appeared similar to uninjected animals. Since virtually 100% of the acrosomal region of spermatids at Steps 9–18 of spermiogenesis was overlain by ES, it was easy to recognize when ES was disrupted by CD. Generally, increasing dosages and longer exposure times caused greater loss of ES, although spermatids within a tubule or in different regions of the

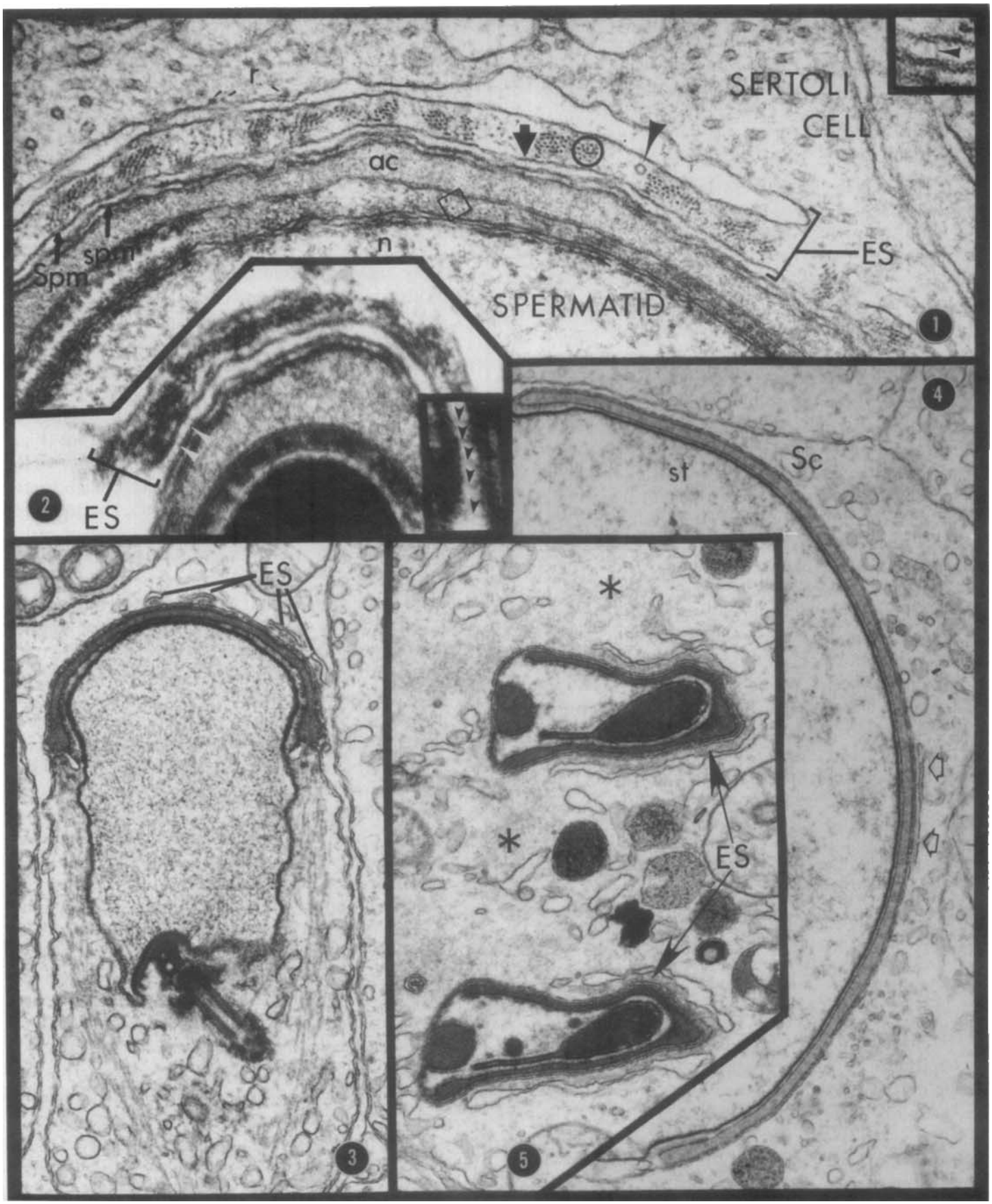

PLATE I.

FIG. 1. The ectoplasmic specialization *(ES)* of an untreated testis appears as a surface specialization of the Sertoli cell, here seen facing a late Step 9 spermatid. Actin filament bundles *(encircled)* and an occasional microtubule *(arrowhead)* are sandwiched between a large saccule of endoplasmic reticulum (containing sparce ribosomes [*r*] and the Sertoli plasma membrane [*Spm*]). The acrosome *(ac)* of the spermatid and the spermatid nucleus *(n)* are closely apposed to the spermatid plasma membrane *(spm)*. Fine fibrillar cell-to-cell linkages *(bold arrow* and *inset)* are occasionally seen. Also indicated is subacrosomal actin *(enclosed* in a *square)*. Osmium-only post-fixation. × 95,000.

FIG. 2. This cytoskeletal preparation (see *Materials and Methods)* of an untreated testis reveals to advantage the cell-to-cell linkages at *ES* sites. Fine fibrils *(white arrowheads* and *inset)* cross the intercellular space between the Sertoli cell and spermatid. Fibrils appear not to be uniformly distributed within the intercellular space. × 136,000.

FIG. 3. After cytochalasin D (CD) treatment (500 μM for 6 h), the Step 11 spermatid illustrated demonstrates normal morphology. However, the *ES* overlying the sperm head is not extensive as in untreated or DMSO controls. The ES appears fragmented into small segments which face the acrosomal region of the spermatid. × 22,000.

FIG. 4. This early Step 9 spermatid *(st)* from a CD-treated (500 μM for 6 h) testis shows a virtual absence of Sertoli cell *(Sc)* ES over a large expanse of its acrosomal surface except at one site *(arrows)* where the ES is poorly represented. × 19,000.

FIG. 5. Two Step 18 spermatids from a CD-treated (500 μM for 6 h) testis show partial loss of *ES*. Amorphous material or "foci" *(asterisks)*, thought to be fragmented actin, appear near the regions of ES loss. × 24,000.

testis of the same animal showed variation in the amount of ES lost.

Vehicle-treated or uninjected animals generally demonstrated a single extensive ES complex overlying the entire acrosomal region. In CD-treated tissues, the complexes were often less extensive and fragmented into multiple complexes (Fig. 3). Frequently, there were areas within the Sertoli cell that showed amorphous densities adjacent to areas where ES was expected to be found (Fig. 5). These amorphous densities were similar in appearance to what has been described as microfilamentous masses or actin foci within cells (Spooner et al., 1971; Miranda and Godman, 1973; Schliwa, 1982). Foci, as they are termed herein, have been considered to be aggregations of disrupted actin, characteristically seen after cytochalasin treatment in the vicinity of the disrupted actin.

Many spermatids which have lost ES show the development of structures that generally resemble tubulobulbar complexes (Russell and Clermont, 1976). The tubulobulbar-like structures were not configured with bulbous dilatations but were similar to those appearing extremely late in spermiogenesis as described by Russell (1979a). They were atypical in that they were commonly cytoplasmic projections containing, in addition, a projection of the acrosome (Figs. 6, 7, and 9, 500 μM for 6 h; Fig. 8, 500 μM for 3 h). As with tubulobulbar complexes, a bristle-coated pit was observed at the distal aspect of the Sertoli invagination (Figs. 7–9).

NBD-P was used as a probe to visualize F-actin of the ES in elongate spermatids at Steps 11–18 of development, where ES was recognized as it conformed to the characteristic elongate shape of the spermatid head. It has been shown that the pattern of ES in the rat is not confused with subacrosomal actin (Masri et al., 1987), which is found within elongate spermatids (Russell et al., 1986b) where Sertoli cell and spermatid are held together.

In vehicle controls, ES F-actin was recognized in epithelial sheet preparations as a moderately bright fluorescent signal seen uniformly along and conforming to the shape of the head region of the cell (Figs. 10 and 12). In CD-treated animals, comparable ES F-actin fluorescence was generally less extensive over the spermatid head. The pattern was not uniformly continuous over the spermatid head, but rather demonstrated a patchy or spotty appearance slightly removed from the spermatid head (Fig. 13). This NBD-P pattern suggested, as transmission-electron micrographs show, that partial disruption of ES was effected. The patchy appearance in some figures may be attributed to nearby fragmented actin (foci), which reacted with NBD-P or actin surrounding tubulobulbar complexes (Fig. 11, see below).

Hypertonic fluids added to the perfusate provoked cell shrinkage and resulted in an exaggeration of the intercellular space between cells. There was, however, a variable response to cell shrinkage in untreated and DMSO-treated tissues as compared with CD-treated animals. Generally, only the basal compartment cells showed shrinkage in untreated and DMSO-treated animals, whereas all germ cells separated from germ cells in CD-treated animals. This response has been attributed to concomitant disruption of the Sertoli cell barrier at Sertoli-Sertoli ES sites after CD treatment (Weber et al., 1988), which allowed rapid access of hypertonic fluids into the adluminal compartment and resulted in cell shrinkage throughout the epithelium. Therefore, to produce equivalent adluminal tonicity changes in DMSO-treated controls, tubular fragments from these controls were incubated in hypertonic fluids to allow access of fluids to adluminally positioned cells via the tubular lumen. Also, the same adluminal shrinkage

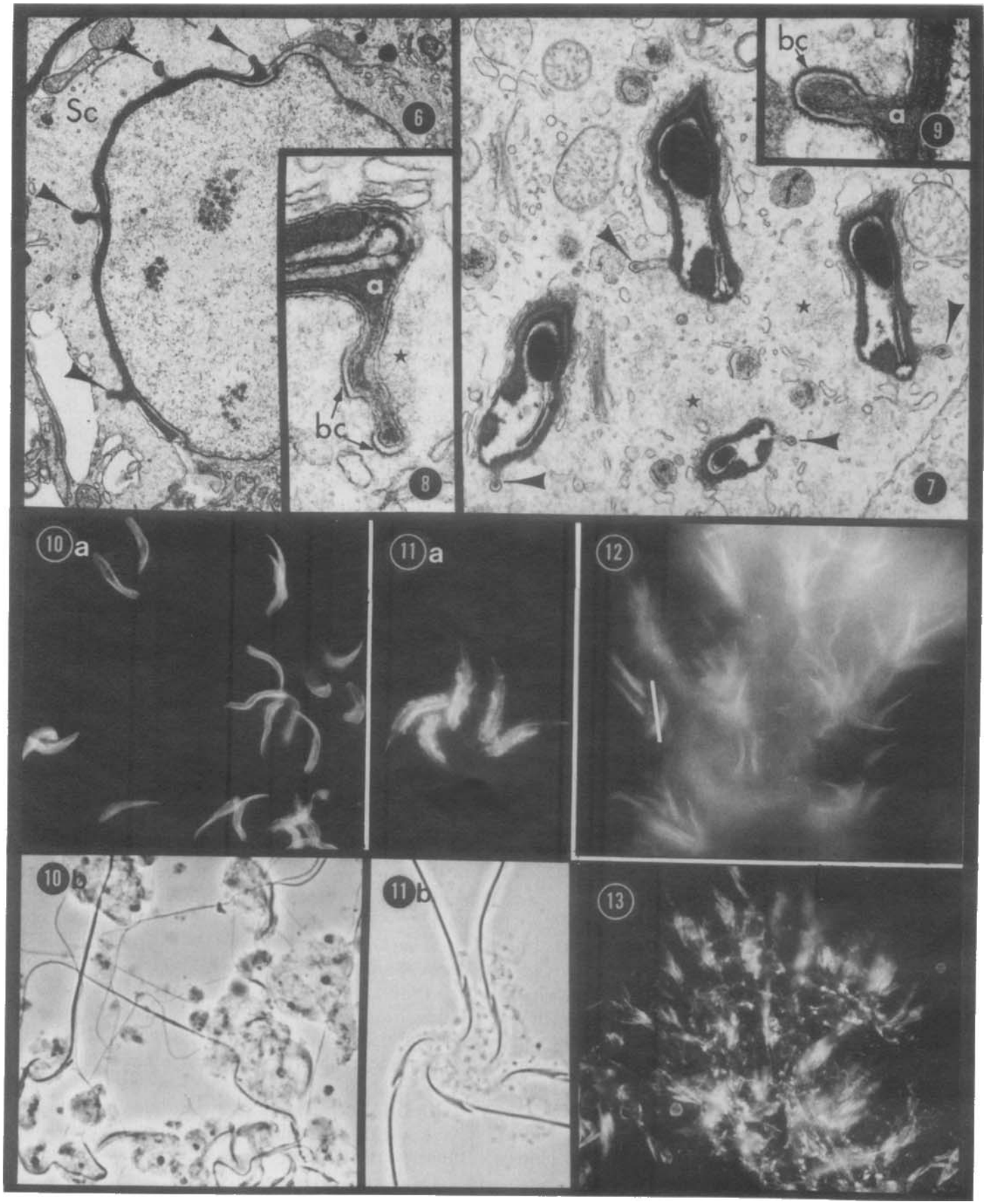

PLATE II.

FIG. 6. In this section, a young Step 9, cytochalasin D (CD)-treated spermatid (500 μM for 6 h) shows a complete absence of Sertoli ectoplasmic specialization *(ES)* at sites where it is normally present over the spermatid head. Tubulobulbar-like structures *(arrowheads)* containing acrosomal protrusions have formed at several sites to indent the Sertoli cell *(Sc)*. These tubulobulbar-like structures have expansions at their tip that are coated pits. × 3200.

FIG. 7. Four Step 17 CD-treated (500 μM for 6 h) spermatids show partial loss of Sertoli ES from their surfaces and "foci" *(stars)* adjacent to the spermatid head. Structures resembling tubulobulbar complexes *(arrowheads)* have developed from the cell surfaces in regions free of ES. The complexes are short protrusions of the spermatid plasma membrane and acrosome, which indent the Sertoli cell. At the depth of the Sertoli cell invagination, a bristle coated pit is noted *(tip of arrowhead)*. × 15,000.

FIGS. 8–9. Tubulobulbar complex-like elements from Step 16 and Step 11 spermatids, respectively, demonstrate bristle-coated *(bc)* areas along the Sertoli cell invagination and at the depth of the invagination. Also indicated (*Fig. 8* only) are suspected actin filaments *(star)* and the acrosomal protrusion *(a)*. Treated with an injection of 500 μM CD and killed 3 and 6 h later, respectively. *Figure 8:* × 32,000; *Figure 9:* × 48,000.

FIGS. 10–13. Nitrobenzoxadiazole-phallacidin (NBD-P) stained *(Figs. 10a, 11a, 12–13)* and selected companion phase micrographs *(Figs. 10b* and *11b)* of vehicle-treated *(Figs. 10* and *12)* and CD-treated testis *(Fig. 11* and *13*, 500 μM for 10 h) showing F-actin localization. In vehicle-treated testis, the ES appears uniformly fluorescent and conforms to the shape of the spermatid head. *Figure 12* is similar to *Figure 10* with the exception that the spermatids remain embedded in a cluster of Sertoli cells (vague fluorescence). In CD-treated testis, the ES is less prominent and spotty *(Fig. 13)*. However, areas that lie along the side of the spermatid head are moderately fluorescent and presumed to be "foci" or actin associated with tubulobulbar complexes *(Fig. 11a)*. ×850.

was provoked (not shown) by use of hypertonic dextrose (10–20%) in the saline wash prior to fixation with glutaraldehyde containing dextrose (10–20%). Regardless of how adluminal shrinkage was obtained, in both normal and DMSO-treated animals, the intercellular space at the Sertoli cell elongate(ing) germ cell interface was exaggerated, except over the head region of spermatids where it was uniformly maintained at ES sites (Fig. 14). Subsequent to CD treatment (300–500 μM) for one-half to twelve hours prior to sacrifice, the elongate(ing) spermatids showed regions of exaggerated intercellular space at sites where ES was missing (Figs. 15–17). Generally, small rounded processes of the Sertoli cell were seen in the vicinity of the spermatid head, whereas in vehicle-treated and untreated animals the spermatid head faced the body of the Sertoli cell (Fig. 14). After CD (not shown) treatment, close cell-to-cell spacing was always seen where ES was present, although, commonly, little ES remained (Figs. 15–17).

Freeze-fracture replicas of the membrane faces of both Sertoli and germ cells in the region where ES was expected to face elongate(ing) spermatids revealed membrane faces to contain apparently randomly situated intramembranous particles of various sizes (Fig. 18) similar to those shown by McGinley et al. (1981). No difference was noted in membrane faces of CD- (not shown) and vehicle-treated animals given 300–500 μM CD up to 12 h post-injection. Due to the inherent difficulties in viewing overlapping membranes in the same plane by using the freeze-fracture technique, it was not possible to determine if membrane faces examined in CD-treated animals were those deficient in ES; however, the number of faces examined suggested that, by probability alone, several ES-deficient membrane faces would have been examined in the survey that was undertaken.

Morphometry was performed to document loss of ES at Stage VIII of the cycle (Table 1). Individual Step 8 spermatids demonstrated (in section) a mean ES length of 2.36 ± 1.2 (SD) μm. After CD treatment, the mean ES length was reduced to 0.28 ± 0.16 μm. The ES length, expressed as a percentage of the acrosome length, was 27.68 ± 13.35 (SD) in vehicle-treated animals and 2.99 ± 1.75 in CD-treated animals. This represented a loss of 88% of the ES.

Morphometry was utilized to determine orientation versus malorientation of spermatids after vehicle and CD treatments (Table 1). In vehicle-control tissues, 0.60% ± 0.02 (SD) of cells were found to be maloriented, whereas after CD (500 μM for 6 h) 3.53% ± 1.62 of cells demonstrated malorientation. An example of malorientation in a CD-treated animal is shown in Figure 19. Generally, where malorientation was observed after CD treatment, there was no evidence (in section) of Sertoli ES anywhere along the acrosome of the maloriented spermatid suggesting complete loss of ES.

DISCUSSION

In the present study, CD was shown to disrupt Sertoli ES actin adjoining the heads of elongate(ing) spermatids. A relationship was demonstrated between the presence of ES actin and the ability of Sertoli cells and germ cells to adhere at sites where ES actin was present. Furthermore, there was an approximately 6-fold increase in maloriented cells in CD-treated versus control animals. These data suggest, but do not prove, a role (probably indirect) for ES

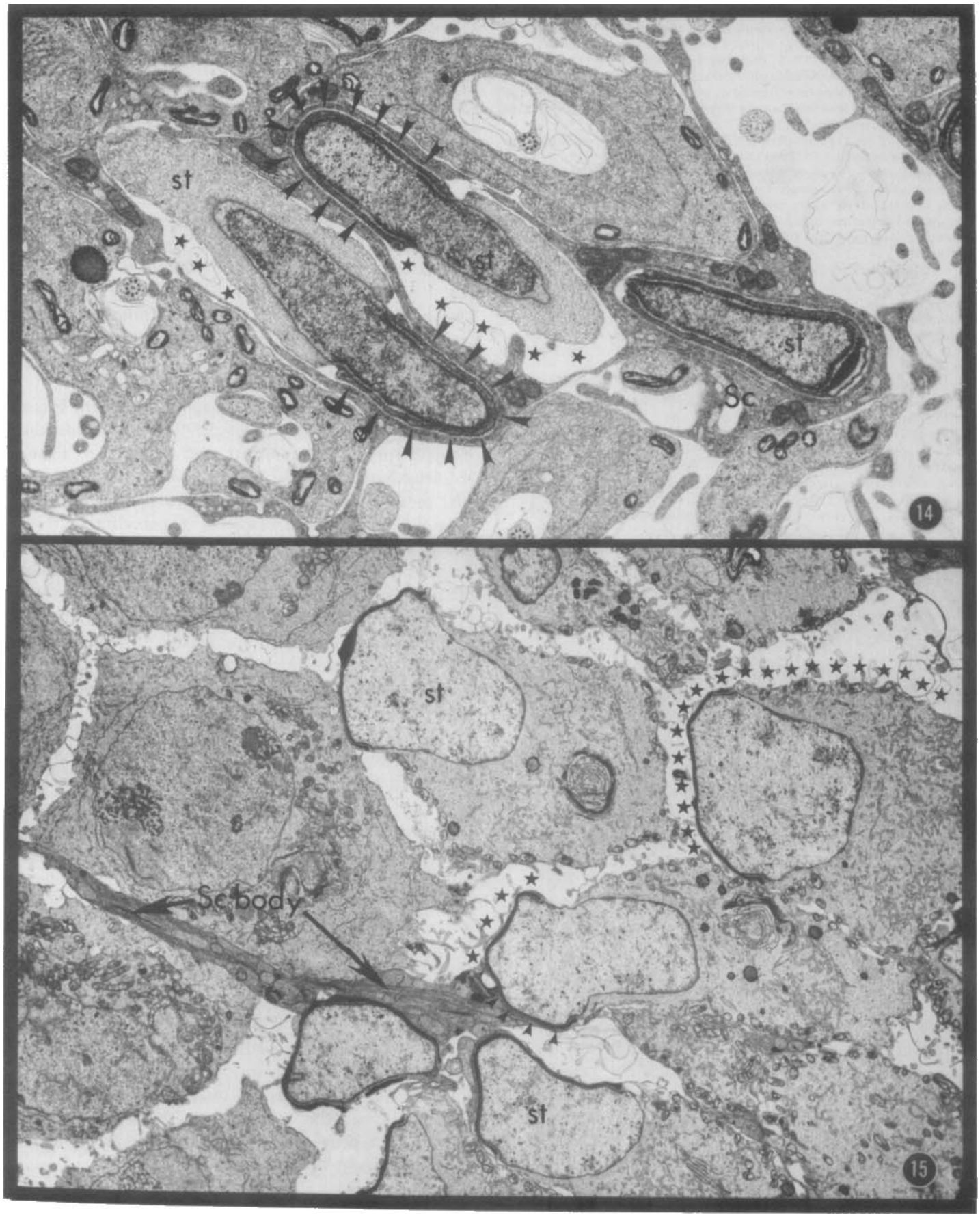

PLATE III.

FIG. 14. This vehicle-treated tissue was perfused-fixed with 10% dextrose in saline prior to introducing glutaraldehyde (containing 10% dextrose). Intercellular spaces are exaggerated between the Sertoli cell and germ cell *(stars)*, except where Sertoli ectoplasmic specialization (ES) is present over the spermatid *(st)* head (see *arrowheads)*. Spermatid heads remain in contact with the body of the Sertoli cell *(Sc)*. × 5600.

FIG. 15. This cytochalasin D (CD)-treated (500 μM for 6 h) tissue was perfused-fixed with fixative containing 10% dextrose. Intercellular spaces *(stars)* are exaggerated between the Sertoli cell *(Sc)* and Step 8 spermatids *(st)* virtually over the entire cell surface, including most of the head of the spermatid. A small amount of ES is present *(arrow)* and, at this site, the Sertoli cell and spermatid are closely apposed. In one area, the body of the Sertoli cell is seen to make contact with portions of the acrosomal region of three Step 8 spermatids. × 4800.

actin in both cell attachment and cell orientation within the seminiferous epithelium.

Evidence now suggests that ES may be associated with the property of cell adhesion as earlier implied in the term "junctional specialization." We believe, however, that the term ES should be retained, since additional functions have been attributed to the ES (Brökelmann, 1963; Ross and Dobler, 1975; Ross, 1976; Russell, 1977; Gravis, 1979; Russell and Peterson, 1985; Sprando and Russell, 1987). It is suggested that the term, ES, henceforth be applied to the entire apparatus, including the elements which traverse the intercellular space to link the two cells together.

The mechanism by which actin could be related to cell-to-cell adhesion is not known at present for any cell system. However, it is well known that actin is found in association with zonula adherens and tight junctions in various epithelia (Hull and Staehelin, 1976; Bentzel et al., 1980; Cereijido et al., 1980; Meza et al., 1980, 1982: Hirokawa and Tilney, 1982; Madara, 1983; Hageman and Kelly, 1984), and its disruption with cytochalasin leads to changes in intramembranous particles (IMPs) forming occluding junction rows as well as accompanying permeability changes (Bentzel et al., 1980; Cereijido et al., 1980; Meza et al., 1980; 1982; Rassat et al., 1982; Madara, 1983; Weber et al., 1988). Thus, it appears that actin, through membrane linkers, may influence the position of integral membrane proteins. The junction studied in this report, unlike that at the interface of Sertoli cells, (Weber et al., 1988) is atypical in that no particular organization of IMPs is revealed upon examination of the plasma membrane faces of either Sertoli or germ cells. Although, in the present report, CD disruption may have caused IMP distribution changes, such changes may have gone unnoticed due to apparent random organization of particles. Also, the unique character of this particular junction, whereby intercellular linkages are not easily visualized (Russell and Peterson, 1985), makes the study of the ES junctions more difficult. It is generally known that actin can be anchored into the cell membrane in a variety of cell types and influence the position of integral membrane proteins (see Jacobson, 1983). ES actin, through membrane links or maintenance of membrane domains, may directly influence the position of membrane protein domains as has been proposed by Vogl et al. (1986) and Masri et al. (1987). An alternate possibility is that actin does not directly influence the position of IMPs, but simply structurally stabilizes the junctional regions. This mechanism would account for weakened intercellular adhesion in CD-treated cells and the apparent lack of change in freeze-fracture replicas of junctional membrane.

That ES is involved in spermatid orientation was initially proposed by Russell (1977), and experimental data subsequently have been collected to support, but not prove, this hypothesis (Russell et al., 1983). In the present report, it has been shown that cells entirely lacking ES (in section) were frequently maloriented. Cells with partial ES were generally oriented properly. Therefore, it appears that a full complement of ES is not necessary for the cell to be maintained in the proper orientation. The data suggest, however, that a complete loss of ES may facilitate malorientation.

Strict orientation of cells appears to be a fundamental feature of spermatid development in mammals and nonmammalian vertebrates. As cells become oriented to the basal aspect or the body of a nearby Sertoli cell, they assume a position that allows the head region of the cell to come to lie deeply with developing crypt of the Sertoli cell with the spermatid tail trailing into the lumen. ES appears to be involved in the initial orientation of spermatids that first occurs at early Step 8 in development in the rat. Once oriented, cells that had elongated and were embedded in deep crypts of the Sertoli cell did not lose their orientation after CD treatment. There are several possible reasons for orientation of germ cells. Orientation may be simply organizational, it may be metabolic, and/or it may be related to development of the mechanism of sperm release and the orderly directioned release of sperm.

Other functions of ES have been proposed which include its timed dissolution near the end of spermio-

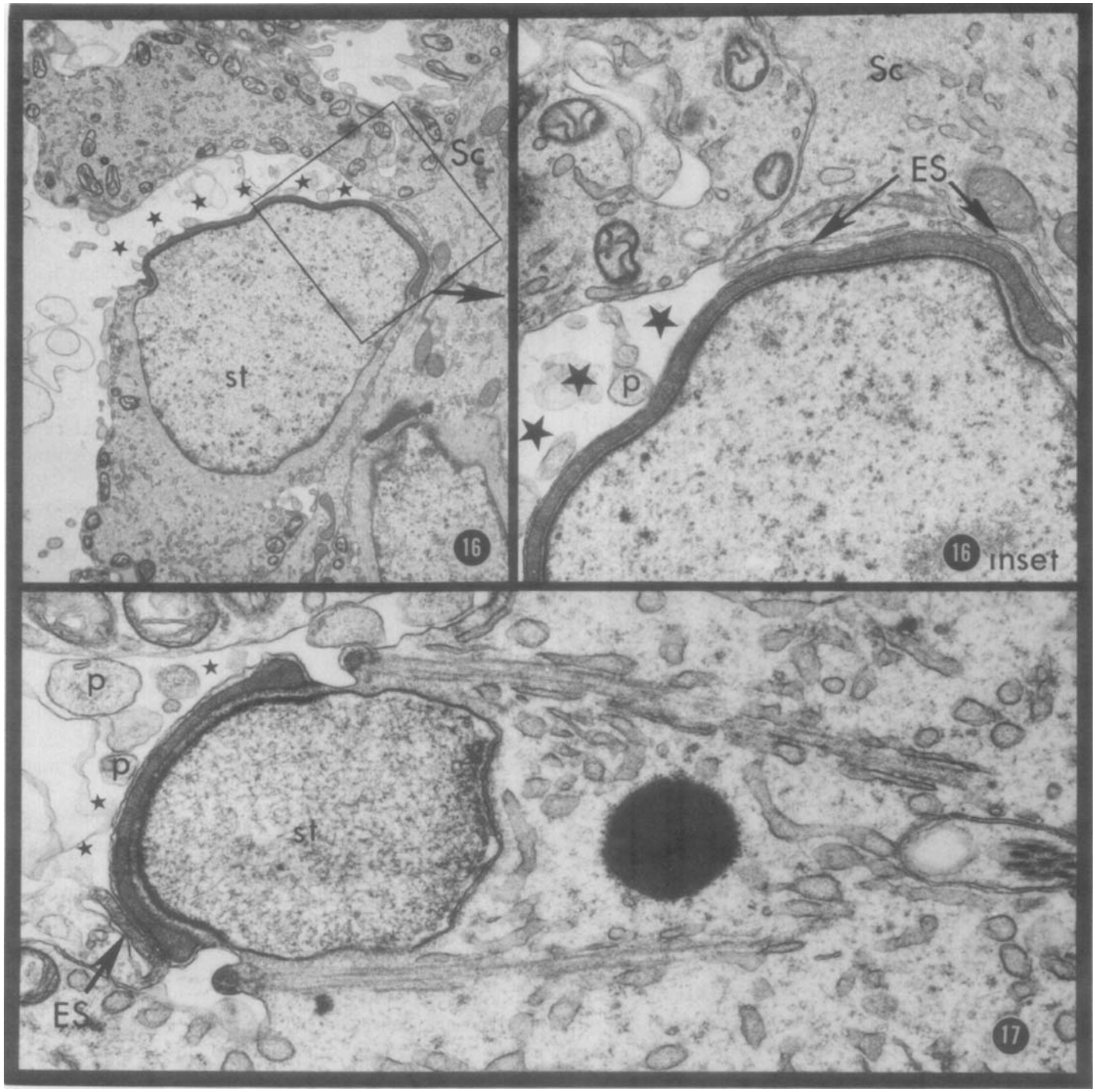

PLATE IV.

FIGS. 16–17. Cytochalasin D (CD)-treated (500 μM for 6 h [*Fig. 16*] and 30 min [*Fig. 17*]), testis perfused with fixative containing 10% dextrose, shows loss of ectoplasmic specialization *(ES)* facing the spermatid *(st)* head. At ES sites, the intercellular space is maintained, whereas at sites where ES is missing, the intercellular space *(stars)* is greatly exaggerated. The magnified *inset* shows this to advantage. Small rounded processes *(p)* of the Sertoli cell *(Sc)* lacking ES are related to the spermatid head where, previous to injection, the body of the Sertoli cell is known to be related to the spermatid at this same position. *Figure 16:* ×6600 (inset×19,800); *Figure 17:* ×26,000.

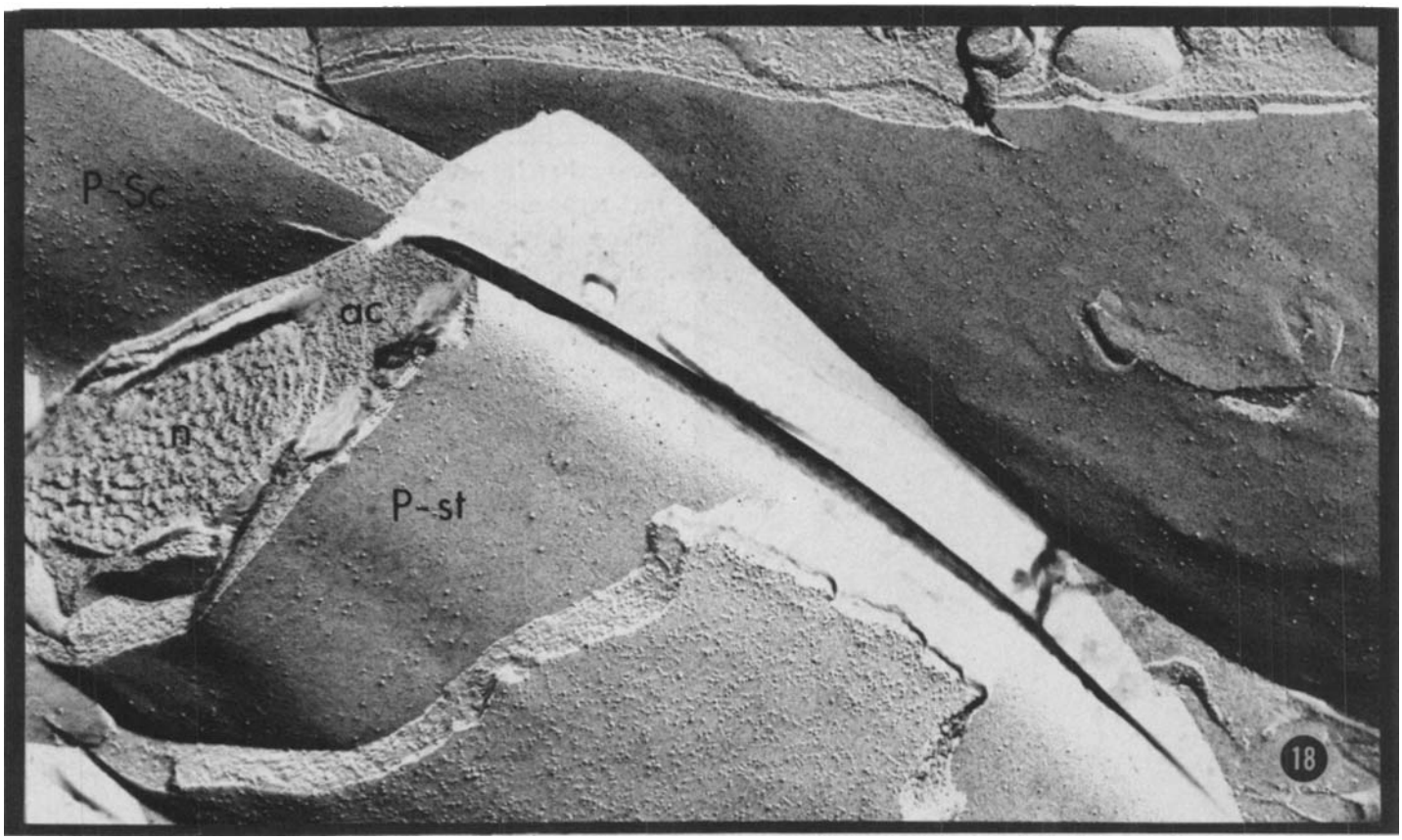

FIG. 18. Replica from a dimethylsulfoxide-treated (killed 12 h later) tissue showing plasma membrane faces *(P)* of Sertoli cells *(Sc)* and elongate spermatids *(st)*. Intramembranous particles are variable in size and apparently randomly distributed in both vehicle- and CD-treatment regimens (not shown). No apparent effect of cytochalasin D on distribution of intramembranous particles was noted. Also indicated are the acrosome *(ac)* and nucleus *(n)*. × 55,000.

genesis, a phenomenon that has been suggested to facilitate the spermiation process through loss of cell-to-cell adhesion. Unfortunately, we were not able to effect 100% ES dissolution for most spermatids to determine if they would be released prematurely; however, we frequently observed that spermatids showing focal ES dissolution developed structures resembling tubulobulbar complexes. The structures that developed after CD treatment resembled tubulobulbar complexes but were without bulbous components

TABLE 1. Morphometric determinations.

Animal	Treatment	Average ES[a] length (μm) per spermatid with acrosome	ES length expressed as a percentage of acrosome length	Mean % of cells showing malorientation
1	Vehicle	3.56	41.03	0.59
2	Vehicle	1.16	14.33	0.62
Mean ± SD		2.36 ± 1.2	27.68 ± 13.35	0.60 ± 0.02
3	CD[b]	0.53	5.81	4.64
4	CD	0.17	1.75	1.79
5	CD	0.13	1.34	2.31
6	CD	0.31	3.06	5.41
Mean ± SD		0.28 ± 0.16	2.99 ± 1.75	3.53 ± 1.52

[a]ES = ectoplasmic specialization.

[b]CD = cytochalasin D.

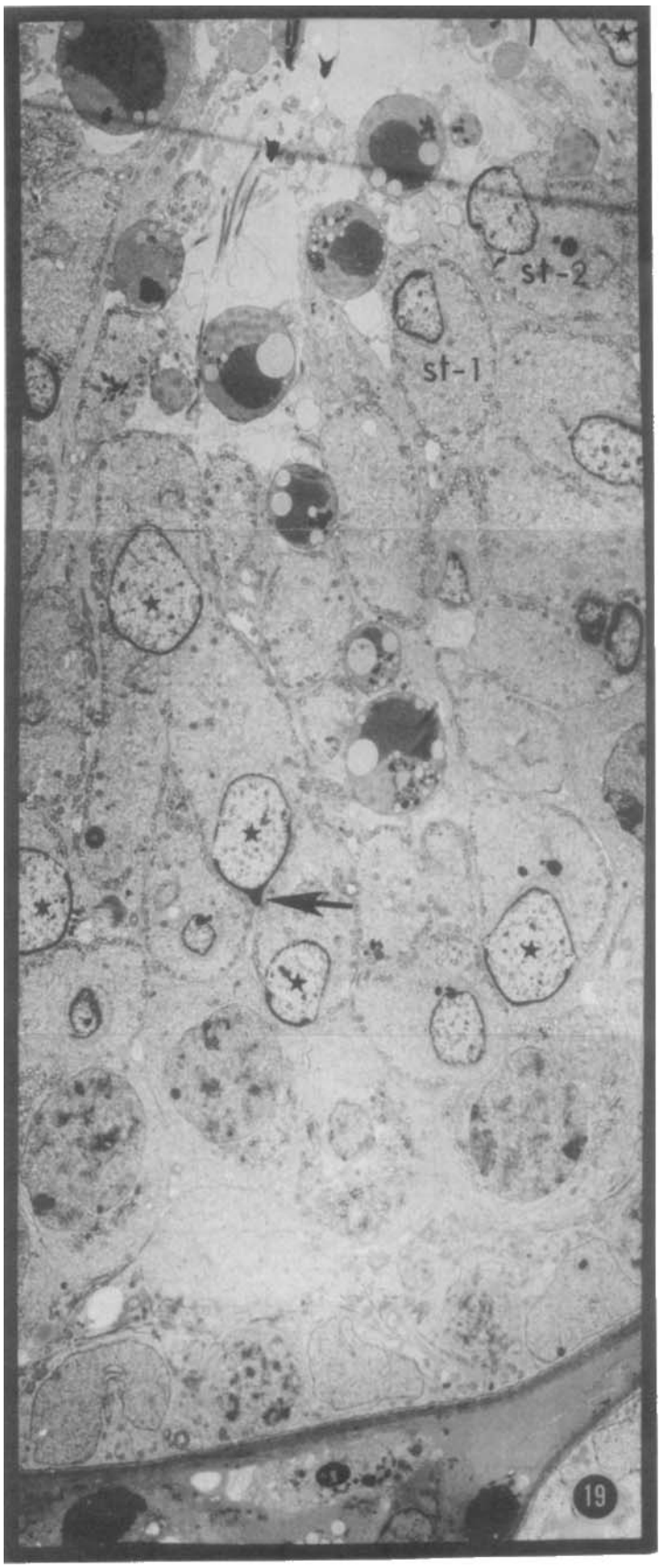

(Russell, 1979a). They also demonstrated a portion of the acrosome that protuded into the complex. That the acrosome also is a component of the tubulobulbar complex-like structure in CD-treated animals may mean that, in spermatids less mature than Step 19, the acrosome and the plasma membrane are tightly linked, but somehow lose this attachment around Step 19. An acrosome-plasma membrane link may also be proposed on the basis of the maintenance of the nuclear eccentricity in Steps 9 and 10 spermatids of normal animals. At this time, the acrosome comes to be closely and evenly spaced from the plasma membrane where it is stabilized along the plasma membrane in one particular region of the cell.

We suggest that when ES is removed from the surface regions of spermatids, tubulobulbar complexes are free to form. This is a process analogous to what happens naturally at Step 19 of spermiogenesis when ES dissolves or is removed (Russell, 1979a; Russell et al., 1980), at first focally and then eventually completely, from a position facing the spermatid head. It has been noted that tubulobulbar complexes form only in those regions where ES has been removed (Russell, 1979a). ES dissolution, either naturally or CD-induced, may present a signal for tubulobulbar complex formation that, in turn, would allow clustering of cell-to-cell attachment units at bristle-coated pits (Russell, 1977). Since cells are attached by cell-to-cell links, a pull on these links would also result in the internalization and degradation of selected areas of the spermatid along with the linking elements. The linking elements seen in cytoskeletal preparations (this report) resemble linking elements connecting the bristle-coated pit to the spermatid tube (Russell and Malone, 1980; Russell and Peterson, 1985).

Clustering of coated-pit receptors containing cell-to-cell linkages of the ES (Russell, 1979a; Russell

FIG. 19. Montage of a portion of a cytochalasin D-treated (500 μM for 6 h) cross-sectioned tubule at late Stage VIII depicting the orientation of numerous Step 8 spermatids. It may be deduced that the majority of spermatids *(stars)* are oriented with their central acrosome region *(arrow)* pointing within 90° of the basal lamina. Two spermatids *(st-1;* st-2) have their acrosome pointing within 90° of the lumen center and are considered maloriented, whereas the remaining spermatids with visible acrosomes are normally oriented. At higher magnification (not shown), no Sertoli ectoplasmic specialization was apparent facing these two spermatids. × 1600.

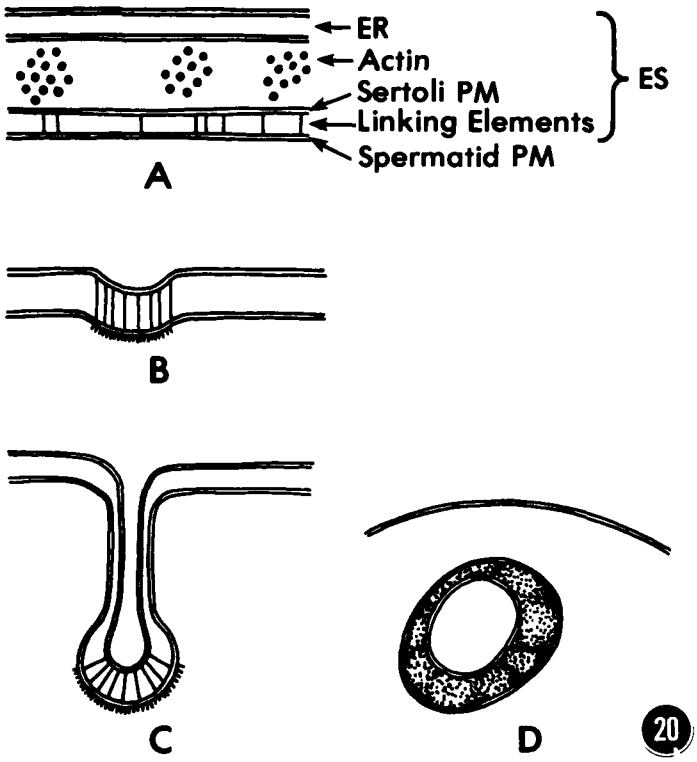

FIG. 20. Diagram summarizing the proposed mechanism by which cell-to-cell linkages are eliminated during the spermiation process: *(A)* Components of the ES are indicated including cell-to-cell linkages which traverse the intercellular space. *(B)* After filament dissolution (either normally or cytochalasin D-induced), linkages are clustered at bristle-coated pits as the result of receptor clustering analogous to the process of receptor-mediated endocytosis. *(C)* Cell-to-cell linkages begin internization and draw the spermatid inward to form a tubulobulbar complex. *(D)* Tubulobulbar complexes are phagocytosed by the Sertoli cell, and cell-to-cell linkages are degraded allowing, the spermatid to separate from the Sertoli cell and be released as a spermatozoon.

and Malone, 1980; Russell and Peterson, 1985) may be analagous to what is occurring in the process of receptor-mediated endocytosis, except that, in this case, the bound ligand molecules are attached at their other ends to the spermatid surface. Internalization of cell-to-cell links, and their subsequent phagocytosis by the Sertoli cell (Russell, 1979a), may be a mechanism to regulate and/or to control the loss of cell adhesion. This would lead to the progressive disengagement of the Sertoli cell from the spermatid and thus be the mechanism for loss of cell attachment during spermiation. It has been noted that the last tubulobulbar complexes to develop do so at the dorsal aspect of the spermatid head, which is also, coincidentally, the final area to lose contact with the Sertoli cell (Russell, 1979a).

Disruption of ES, whether at the interface of Sertoli cells and germ cells, or at the level of the Sertoli cell barrier (Weber et al., 1988), appears to affect cell-to-cell interaction. It has been shown that tubulobulbar complexes at the level of the Sertoli cell barrier are important in disposal of junctional elements (both occluding and gap junctions: Russell, 1979b). In the present report, we suggest that spermatid-Sertoli tubulobulbar complexes perform a similar function, although the junctional elements at this site are of an unconventional variety. Such a hypothesis (diagrammed in Fig. 20) awaits further experimental testing.

ACKNOWLEDGMENTS

Thanks are due to Dr. James E. Weber for assisting in tissue preparation and Ms. Marlene Fink and Ms. Marion Cathey for their help in typing the manuscript.

REFERENCES

Bentzel CJ, Hainau B, Ho S, Hui SW, Edelman A, Anagnostopoulos T, Beneditti EL, 1980. Cytoplasmic regulation of tight-junction permeability: effects of plant cytokinins. Am J Physiol 239: C75–C89

Brökelmann J, 1963. Fine structure of germ cells and Sertoli cells during the cycle of the seminiferous epithelium in the rat. Z Zellforsch Microsk Anat 59:820–50

Cereijido M, Ehrenfeld J, Meza I, Martinez-Palomo A, 1980. Structural and functional membrane polarity in cultured monolayers of MDCK cells. J Membr Biol 52:147–59

Fawcett DW, 1979. Comparative aspects of the organization of the testes and spermatogenesis. In: Alexander NJ (ed.), Animal Models for Research on Contraception and Fertility. New York: Harper and Row, pp. 84–104

Flickinger C, Fawcett DW, 1967. The junctional specializations of Sertoli cells in the seminiferous epithelium. Anat Rec 158:207–21

Franke WW, Grund C, Fink A, Weber K, Jockusch BM, Zentgraf A, Osborn M, 1978. Location of actin in the microfilament bundles associated with the junctional specializations between Sertoli cells and spermatids. Biol Cell 31:7–14

Gravis CJ, 1979. Cytochemical localization of cations in the testis of the Syrian hamster, utilizing potassium-pyroantimonate. Am J Anat 154:245–66

Gravis CJ, Yates RD, Chen I, 1976. Light and electron microscopic localization of ATPase in normal and degenerating testes of Syrian hamsters. Am J Anat 147:419–32

Hageman GS, Kelly DE, 1984. Fibrillar and cytoskeletal substructure of tight junctions: analysis of single-stranded tight junctions linking fibroblasts of the lamina fusca in hamster eyes. Cell Tissue Res 238:545–57

Hirokawa N, Tilney LG, 1982. Interactions between actin filaments and between actin filaments and membranes in quick-frozen and deeply etched hair cells of the chick ear. J Cell Biol 98:249–61

Hull BE, Staehelin LL, 1976. Functional significance of the variations in the geometrical organization of tight junction networks. J Cell Biol 68:688–704

Jacobson BS, 1983. The interaction of the plasma membrane with the cytoskeleton: an overview. Tissue Cell 15:829–52

Leblond CP, Clermont Y, 1952. Definition of the stages of the cycle of the seminiferous epithelium in the rat. Ann NY Acad Sci 55: 548–73

Madara JL, 1983. Increases in guinea pig small intestinal transepithelial resistance induced by osmotic loads are accompanied by rapid alterations in absorptive-cell tight-junction structure. J Cell Biol 97:125–36

Masri BA, Russell LD, Vogl AW, 1987. Distribution of actin in spermatids and adjacent Sertoli cell regions of the rat. Anat Rec 218: 20–26

McGinley DM, Posalaky Z, Porvaznik M, 1981. Membrane associations between subsurface cisternae of endoplasmic reticulum and the plasma membrane of rat Sertoli cells. Tissue Cell 13:337–47

Meza I, Ibarra G, Sabanero M, Martinez-Palamo A, Cereijido M, 1980. Occluding junctions and cytoskeletal components in cultured transporting epithelium. J Cell Biol 87:746–54

Meza I, Sabanero M, Stefani E, Cereijido M, 1982. Occluding junctions in MDCK cells: modulation of transepithelial permeability by the cytoskeleton. J Cell Biochem 18:407–21

Miranda AF, Godman GC, 1973. The effects of cytochalasin D on differentiating muscle in culture. Tissue Cell 5:1–22

Nicander L, 1967. An electron microscopical study of cell contacts in the seminiferous tubules of some mammals. Z Zellforsch Miscrosk Anat 83:375–97

Rassat J, Robenek H, Themann H, 1982. Cytochalasin B affects the gap and tight junctions of mouse hepatocytes *in vivo*. J Submicrosc Cytol 14:427–39

Romrell LF, Ross MM, 1979. Characterization of Sertoli cell-germ cell junctional specializations in dissociated testicular cell. Anat Rec 193:23–42

Ross M, Dobler H, 1975. The Sertoli cell junctional specializations and their relationship to the germinal epithelium as observed after efferent ductule ligation. Anat Rec 183:267–92

Ross MH, 1976. The Sertoli cell junctional specialization during spermiogenesis and at spermiation. Anat Rec 186:79–104

Russell L, 1977. Observations on rat Sertoli ectoplasmic ('junctional') specializations in their association with germ cells of the rat testis. Tissue Cell 9:475–98

Russell LD, 1979a. Further observations on tubulobulbar complexes formed by late spermatids and Sertoli cells in the rat testis. Anat Rec 194:213–32

Russell LD, 1979b. Observations on the inter-relationships of Sertoli cells at the level of the blood-testis barrier: evidence for formation and resorption of Sertoli-Sertoli tubulobulbar complexes during the spermatogenic cycle. Am J Anat 155:259–80

Russell LD, Burguet S, 1977. Ultrastructure of Leydig cells as revealed by secondary tissue treatment with a ferrocyanide-osmium mixture. Tissue Cell 9:751–66

Russell LD, Clermont Y, 1976. Anchoring device between Sertoli cells and late spermatids in rat seminiferous tubules. Anat Rec 185: 259–78

Russell LD, Lee IP, Ettlin R, Peterson RN, 1983. Development of the acrosome and alignment, elongation and entrenchment of spermatids as seen in procarbazine treated rats. Tissue Cell 15:615–26

Russell LD, Malone J, 1980. A study of spermatid-Sertoli tubulobulbar complexes and selected mammals. Tissue Cell 12:263–85

Russell LD, Myers P, Ostenburg J, Malone J, 1980. Sertoli ectoplasmic specializations during spermatogenesis. In: Steinberger E, Steinberger A (eds.), Testicular Development, Structure, and Function. New York: Raven Press, pp. 55–63

Russell LD, Peterson RN, 1985. Sertoli cell junctions: morphological and functional correlates. Int Rev Cytol 94:177–211

Russell LD, Sprando RL, Killinger J, Wilzcynski S, Thomasson RW, Tolzmann G, Burt A, 1986a. A simple technique for perfusion of the rat testis through the heart. J Androl 7:P32

Russell LD, Weber JE, Vogl AW, 1986b. Characterization of filaments within the subacrosomal space of rat spermatids during spermiogenesis. Tissue Cell 18:887–98

Schliwa M, 1982. Action of cytochalasin D on cytoskeletal networks. J Cell Biol 92:79–91

Spooner BS, Yamada KM, Wessells NK, 1971. Microfilaments and cell locomotion. J Cell Biol 49:595–613

Sprando RL, Russell LD, 1987. A comparative study of Sertoli cell ectoplasmic specialization in selected non-mammalian vertebrates. Tissue Cell 19:479–93

Toyama Y, 1976. Actin-like filaments in the Sertoli cell junctional specializations in the swine and mouse testis. Anat Rec 186: 477–92

Vogl AW, Grove BD, Lew GJ, 1986. Distribution of actin in Sertoli cell ectoplasmic specialization and associated spermatids in the ground squirrel testis. Anat Rec 215:331–41

Vogl AW, Soucy LJ, 1985. Arrangement and possible function of actin filament bundles in ectoplasmic specializations of ground squirrel Sertoli cells. J Cell Biol 100:814–25

Weber JE, Turner TT, Tung KSK, Russell LD, 1988. Microfilament involvement in maintenance of the Sertoli cell barrier. Am J Anat 182:130–47